Plasmon excitation in sets of nanoscale cylinders and spheres

S. E. Sburlan,* L. A. Blanco,† and M. Nieto-Vesperinas‡
Instituto de Ciencia de Materiales de Madrid, Consejo Superior de Investigaciones Científicas, Cantoblanco, 28049 Madrid, Spain
(Received 8 September 2005; published 4 January 2006)

By means of the boundary element method, we calculate and interpret the spectral lineshapes and near field spatial distributions of sets of a few nanospheres and nanocylinders on illumination close to the plasmon polariton excitation wavelength. This collective behavior is studied versus that of one isolated particle. Comparisons with results from previous experiments are done. As far as cylinders are concerned, our procedure goes beyond former calculations based on the quasi-electrostatic approximation and, hence, it is exact. It allows to address mixtures of a few of these particles with different sizes providing the configuration possesses axial symmetry. In particular, configurations with nanoantenna behavior are discussed. Finally, we discuss in terms of the direction of propagation and polarization of the incident wave, both the spectral and spatial field distributions of a chain of three self-similar metallic nanospheres whose plasmon eigenmodes were previously analytically obtained and whose properties of nanofocusing were predicted.

DOI: 10.1103/PhysRevB.73.035403 PACS number(s): 78.67.−n, 73.20.Mf, 42.25.Fx

I. INTRODUCTION

Efficient concentration and intensity enhancement of light both in space at the nanoscale[1,2] and in the spectral range[3–5] are proposed as promising means of optical sensing and characterization[6–11] and signal transmission,[12–14] of interest in physics, chemistry, and biology. In this connection, the excitation of eigenmodes of micro- and nanoparticles is a subject of intensive research in order to achieve those objectives. In particular, surface plasmon polaritons in metallic particles are known to give rise to those field characteristics. In the laboratory, the plasmonic excitations of metal nanospheres have been exploited in order to manipulate[15,16] and enhance the Raman signal emitted by biological molecules.[7] In addition, there has also been an attempt to achieve focusing of the local field by means of a chain of silver nanospheres of selfsimilar sizes in vacuum.[17] In that work the eigenmodes of the system, that is, the surface plasmon modes, are derived as the solution of a self-consistent equation. However, their response to an incident electromagnetic wave has not yet been addressed. A strong enhancement of the electromagnetic field in the regions between the spheres, especially between the smallest spheres, is predicted. Hence, this system can be used as a nanometric lens in the ultraviolet regime.

Plasmon resonances of spheres and infinite cylinders have been extensively studied using Mie theory.[18,19] Calculations for finite cylinders, however, are often performed in the Rayleigh limit (where the size of the particle is much smaller than the wavelength), assuming a static electric field.[20,21] Recently, it was determined that gold nanorods exhibit a drastic reduction of plasmon damping compared to nanospheres.[21] It was shown that the plasmon oscillations in cylindrical particles incur fewer losses which allow for a longer lifetime and a narrower linewidth. This can make them more effective for experimental purposes, thus it is important to analyze their behavior under different configurations using numerical methods.

In this work, we make use of the boundary element method (BEM),[22] in which the surfaces of the objects are discretized and Maxwell's equations are solved for the surface charge and current densities induced at the interfaces by the field source (in our case, incident plane waves). This numerical procedure allows us to calculate the near and far fields for configurations with axial symmetry in an incident field and to go beyond the Rayleigh limit. In Sec. II, we begin be analyzing the plasmon excitations of isolated gold cylinders in different size ranges. In Sec. III, we study systems of two and three gold cylinders with distinct resonance frequencies. We explore the effects of coupling among the plasmon oscillations on the linewidths and amplification of the individual particle signals, also addressing situations of nanoantenna behavior. In Sec. IV, we present results for ensembles of two spheres and one cylinder which exhibit a significant cooperative effect among the plasmons leading to a dramatic amplification in the far-field spectrum. In Sec. V we also study the system formed by three selfsimilar silver spheres in order to verify the effect of the calculated eigenmodes and field enhancement in[17] for different polarizations and incidence angles. Finally, in Sec. VI we present a summary of the results obtained and give our conclusions.

II. GEOMETRY-DEPENDENT SURFACE PLASMON EXCITATIONS IN FINITE ISOLATED CYLINDERS

We begin by studying individual gold nanorods in the size ranges analyzed in the experiments described in Ref. 21. The index of refraction of the surrounding medium is 1.5 as used therein. In order to avoid numerical convergence problems, we model the cylinder with a slight curvature near the top (see inset in Fig. 1), and calculate the far field scattering intensity (that is, the total number of photons from the light source scattered by our system in all directions) of isolated gold cylinders with different lengths and diameters over a range of frequencies. The source is a plane wave incident from the lateral direction and polarized with electric vector direction along the long axis of the cylinder. We use the bulk values for the refractive index of gold given in Ref. 23. Figure 1 illustrates the dependence of the plasmon resonance on

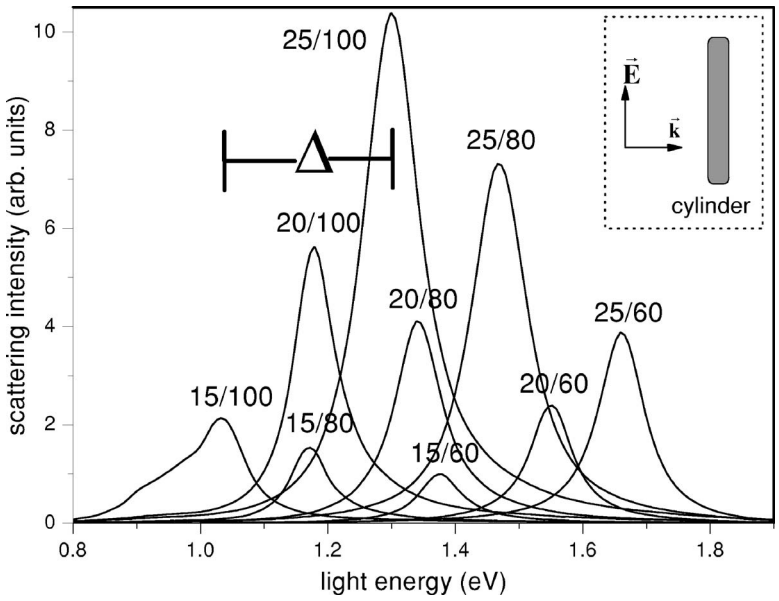

FIG. 1. Light-scattering spectra in isolated gold nanorods of different sizes (diameter/length in nm). The inset shows the directions of propagation and polarization of the incident plane wave. The index of refraction of the surrounding medium is 1.5. Δ denotes the energy shift for two resonance peaks corresponding to cylinders of the same length.

cylinder diameter and length. The scattering intensities are given in arbitrary units, but are plotted in terms of relative values in all forthcoming figures. We will indistinctly use the terms "energy" and "frequency", both expressed in units of eV, taking into account the well known quantum equivalence: 1 eV=2.418×10^{14} Hz.

We note in Fig. 1 that as the length of the cylinders increases for a fixed radius, the scattering amplitude increases and the resonance frequency decreases. We anticipate the increase in scattered light for longer cylinders due to the greater number of oscillating electrons. The linewidths [full width at half maximum (FWHM)] vary only slightly (between 0.08 and 0.13 eV) for all cylinders. Therefore the decrease in resonance frequency with increasing length leads to a lower quality factor $Q=E_{\mathrm{res}}/\Gamma$ (where E_{res} denotes the incident photon energy at which there is plasmon excitation and therefore the scattering efficiency reaches a peak, and Γ is the FWHM of the resonance line), for longer cylinders. For the cylinders in Fig. 1, we find the same dependence of FWHM and Q on the frequency as reported in Ref. 21 below 1.8 eV.

In addition, we observe in Fig. 1 an increase in both the scattering intensity and resonance frequency as the diameter increases. For cylinders of the same length but different diameters, a significant shift in the resonance frequency is found. Since the plasmon oscillations are along the axis of the cylinder, this sensitivity to the cylinder width is surprising. Indeed, we find that if we increase the dimensions of the cylinders by a factor of 10, the dependence on the width disappears, and only the length determines the position of the plasmon resonance. Figure 2 illustrates this result for cylinders with dimensions in the micrometer range. We note only a slight decrease in the peak height as the diameter decreases. Furthermore, the resonances now occur at much lower frequencies, and the scattering amplitude is much greater as we would expect for larger objects.

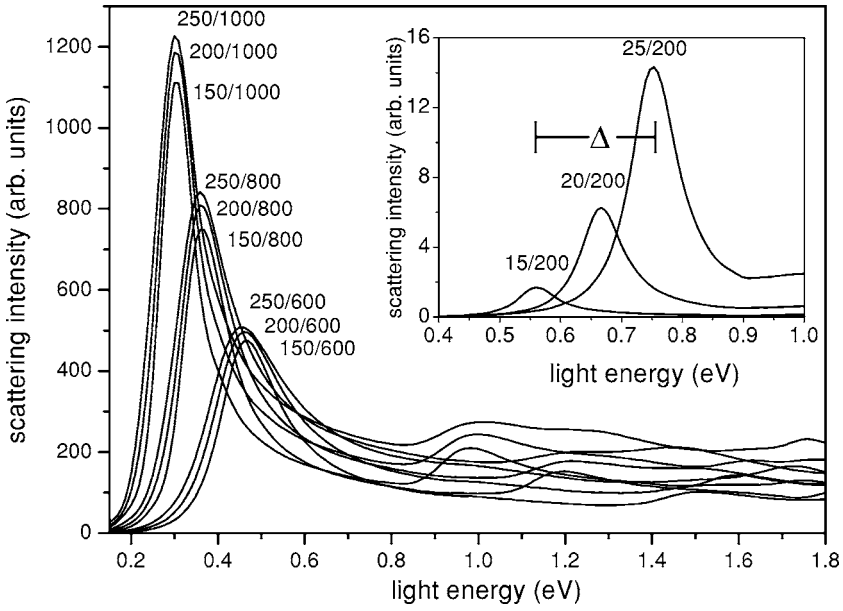

FIG. 2. Light-scattering spectra in isolated gold nanorods. Same conditions as Fig. 1 are used but the dimensions of the cylinders have been increased by 10. Inset: Three isolated cylinders with small diameter and resonances below 1 eV. Δ denotes the energy shift for two resonance peaks corresponding to cylinders of the same length.

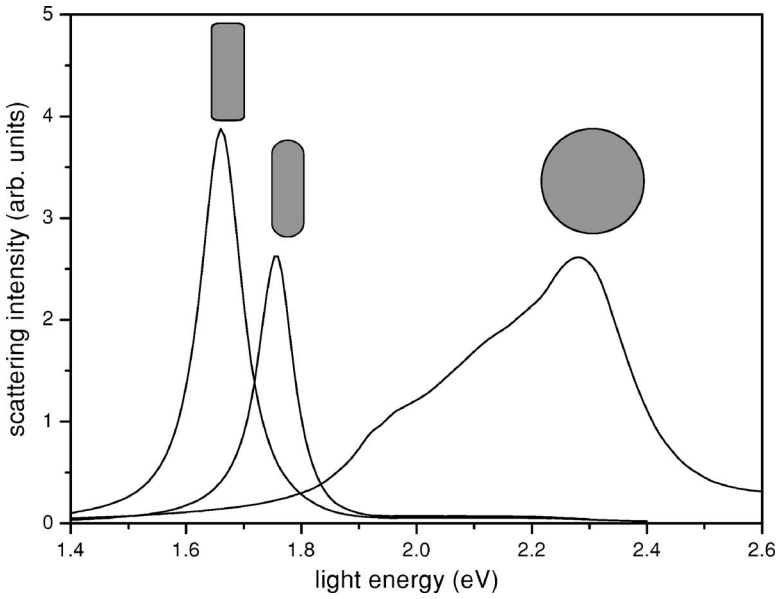

FIG. 3. Light-scattering spectra of an isolated gold nanorod (diameter=25 nm, height=60 nm) with straight and rounded edges and an isolated gold sphere (diameter=60 nm). The index of refraction of the surrounding medium is 1.5.

In order to explain these effects, we must consider both the object geometry as well as the material properties. From the behavior of the dielectric function of gold,[23] we know that the medium is strongly absorbing below 1 eV. At these frequencies, the field cannot penetrate into the medium and the plasmon oscillations are highly localized on the lateral surface. Also, because the cylinders in Fig. 2 have large diameters, the surface plasmon modes are not affected by Coulomb repulsions among the electrons on opposite surfaces. In contrast, because the rods in Fig. 1 have smaller diameters, there can exist electronic forces inside the cylinder that perturb the plasmonic oscillation. Furthermore, because gold is less absorbing at these frequencies, the field can penetrate inside the material and excite electrons within the volume of the cylinder. Thus the combination of smaller dimensions and lower absorption leads to a bulk effect which significantly alters the long axis mode in nanorods of the same length but different diameters.

Further evidence of this is provided in the inset in Fig. 2, which depicts three cylinders with diameter/length 15/200, 20/200, and 25/200 nm, with resonances below 1 eV. We indicate with Δ the difference in frequency between the smallest and largest peak, and note that the resonances occur much closer to one another ($\Delta=0.16$ eV) than in Fig. 1 ($\Delta=0.28$ eV). Nevertheless, we continue to see a strong difference in peak height as in Fig. 1. This suggests that as we increase the length of the rod, the position of the resonance no longer depends on radius, because we shift into a regime of greater absorption where the plasmon is confined to the surface. In addition, increasing the radius further reduces electronic interactions and collisions within the material, leading to a smaller difference in peak height as in Fig. 2. Repeating the calculations with larger cylinders whose resonance frequencies are below 1 eV (dimensions 45/300, 60/300, and 75/300 nm) confirms these trends.

Sönnichsen *et al.*[21] have experimentally measured the light scattering spectra of a single gold sphere (diameter =60 nm) and cylinder and observed that the dephasing time (and hence Γ^{-1}) of cylinders is much larger than that of spheres. Figure 3 reproduces the light scattering spectra for the cylinder and sphere measured in.[21] While the exact dimensions of the cylinder are not given in Ref. 21, we use a rod with diameter 25 nm, and length 60 nm, because its resonance frequency is close to the one observed in,[21] and it is within the size range reported therein. The peaks on the left in Fig. 3 correspond to the cylinder modeled with two different degrees of curvature at the ends. The smaller peak is for the cylinder whose ends are completely rounded, while the taller peak has ends that are only slightly curved around the corners. We obtain resonance frequencies of 1.76 eV (rounded) and 1.66 eV (curved) for the cylinder, and 2.27 eV for the sphere. The resonant frequencies reported in Ref. 21 are 1.82 eV and 2.19 eV for the cylinder and sphere respectively. Differences in the observed and calculated resonance frequencies for the sphere are most likely due to imperfections in the particle geometry used in the experiment. Indeed, we see that for the cylinder, there is a significant shift in the resonance when round edges are used. Based on Fig. 1, we can interpret the result of rounding the edges as shortening the length of the cylinder—the peak height decreases and the resonance shifts to higher frequencies. The difference due to rounded edges illustrates the sensitivity of plasmon resonances to the object's geometry. Electrons can "sense" the boundaries of the object and adjust their collective oscillations accordingly. (cf. Ref. 24, Sec. 12.1) Using rounded edges better approximates the actual nanorods used in experiments where straight edges are difficult to fabricate.

III. SELECTIVE AMPLIFICATION IN SYSTEMS OF THREE INTERACTING CYLINDERS

We will now present the results obtained when several nanoparticles are placed in close proximity to each other. On the one hand, studying configurations of several particles is of interest because they provide insight into the common laboratory conditions in which many particles are simultaneously observed. Also, special arrangements of a few particles may exhibit resonant structures with characteristics

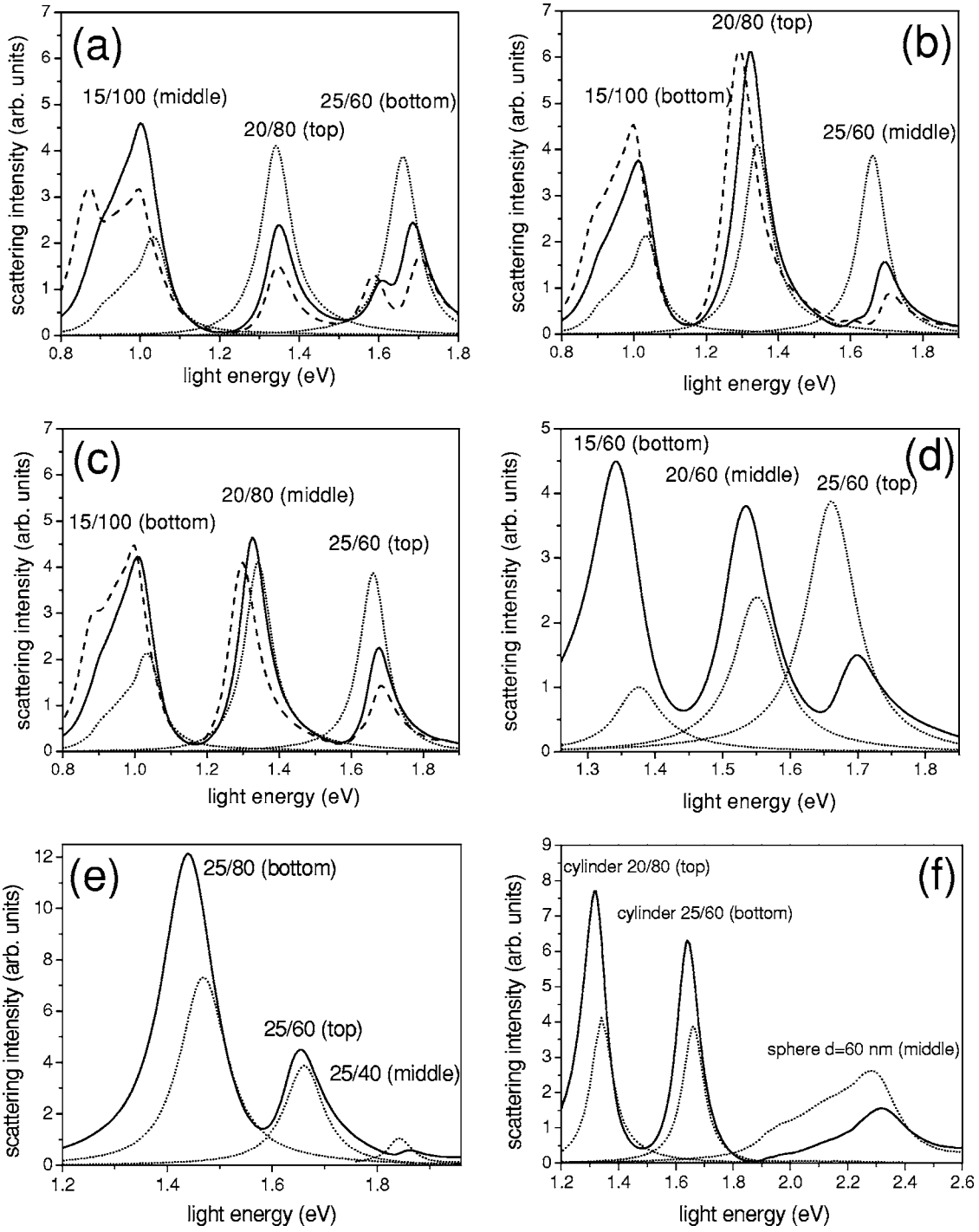

FIG. 4. (a)–(c) Light scattering spectrum for three gold cylinders (15/100, 20/80, 25/60) interacting head to head with a separation of 20 nm (solid line) and 10 nm (dashed line) between them, and light scattering spectra for each isolated cylinder (dots). (d) and (e) Light scattering spectrum for three cylinders of the same length (15/60, 20/60, 25/60) and diameter (25/80, 25/60, 25/40) with a separation of 20 nm (solid) and isolated (dots). (f) Light scattering spectrum for a sphere between two cylinders (solid) and for each isolated particle (dots). In each case, the index of refraction of the surrounding medium is 1.5.

similar to those of an antenna.[25] We model three cylinders with different dimensions (diameter/height in nm=15/100, 20/80, 25/60) aligned head to head in a medium with index of refraction 1.5. The incident plane wave is polarized with the electric vector along the long cylinder axis. We choose these cylinders because of the relatively wide separation between their plasmon resonance frequencies, and wish to observe the effects of plasmon coupling between cylinders on the linewidth and resonance frequency. We calculate the far field scattering spectra of these interacting cylinders in three different configurations, each time placing a different cylinder in the middle. Figures 4(a)–4(c) show the scattering intensities calculated for the three cases with a gap of 20 nm (solid line) and 10 nm (dashed line) between each of the

cylinders. The dotted lines are the scattering spectra for each isolated cylinder (Fig. 1) plotted for comparison.

The scattering spectrum of the interacting cylinders retains the important features of the isolated cylinder spectra. In particular, the plasmon resonance of each individual cylinder remains clearly distinguishable. Each cylinder "lights up" at its respective frequency as it would if it were alone. However, light scattered by the oscillating electrons, as well as the Coulomb forces induced among the cylinders give rise to the observed differences between the collective spectrum and the spectra of each isolated cylinder. The shifts in resonance frequency fall between 0 and 0.04 eV and always occur towards higher energies for the 25/60 cylinder, and lower energies for the other two. With respect to the linewidth, we calculate, in general, a broadening of the peak (1–45 %). While the 15/100 cylinder is clearly the most susceptible to line broadening, we observe in some cases a *narrower* linewidth for the other two cylinders. As a rule, we expect interacting particles to incur greater losses that serve to shorten the plasmon lifetime. Based on our results however, we also allow for the possibility that the electron oscillations in neighboring particles can couple constructively in certain cases, prolonging the duration of the plasmon oscillation.

Indeed, another striking result is the selective amplification of the scattering intensities of the cylinders. In all three cases, the signal from the 15/100 cylinder is amplified by a factor of approximately 2. In contrast, the scattering intensity of the 25/60 cylinder is always significantly diminished in the presence of the other two. We find that the signal from the 20/80 cylinder is both amplified and diminished, depending on its relative position. We can explain these effects with the driven oscillator model (cf. Ref. 24, Sec. 9.1): When one cylinder oscillates at its resonance frequency, it induces plasmonic oscillations in the neighboring particles. If the resonant cylinder drives its neighbors at a higher frequency than their own resonances, they will oscillate out of phase producing destructive interference in the far field. In contrast, driving the cylinders at lower frequencies yields constructive interference because their relative phase difference is zero.

With this model, we can explain why the signals from the 15/100 cylinder and the 25/60 cylinder are amplified and attenuated in all cases: At 1.04 eV, the 15/100 cylinder drives the other two cylinders at a lower frequency than their own resonances. Therefore, the light emitted by all three particles will interfere constructively, producing an amplification at 1.04 eV. This amplification is present regardless of the cylinder position, because it is always next to a neighbor with a higher resonance. The reverse is true for the 25/60 cylinder: its neighbors always oscillate out of phase because of their lower resonance frequencies. An interesting case is the 20/80 cylinder—its signal is attenuated in Fig. 4(a), where it is placed above the 15/100 cylinder. At 1.34 eV, it drives the 15/100 cylinder with a higher frequency which leads to destructive interference. However, in Fig. 4(b), we find that its signal is attenuated because of its proximity to a cylinder with higher resonance (25/60). Finally, in Fig. 4(c), the cylinder is placed in the middle of the other two. Because of the two competing effects, we note only a slight amplification for a separation of 20 nm which is further reduced when the cylinders are brought within 10 nm. These results are consistent with the driven oscillator model and suggest that a particle immediate neighbor has the greatest impact on the amplification or attenuation of that particles signal.

When we bring the cylinders within 10 nm, we observe in Fig. 4(a) splitting of the resonances of the 15/100 and 25/60 cylinders. This splitting, caused by plasmon coupling between neighbor resonant particles as a result of the interaction between the multipolar modes of each individual cylinder, is known and had been observed in spheres.[26]

In Fig. 4, we also show the results obtained for cylinders of the same length (d) and diameter (e). In (d), the two cylinders with lower resonance frequency are amplified while the one with the highest resonance is attenuated. In (e), we achieve a small enhancement of the signal from the 25/60 cylinder by placing it next to one with higher resonance frequency (25/40). In this case, the peak of the 25/40 cylinder almost disappears. Finally, in Fig. 4(f), we model a sphere of diameter 60 nm between two cylinders. Since the sphere resonates at the greatest frequency, its signal is attenuated, while the peaks of the cylinders are amplified. Again, these results are consistent with the driven oscillator model, and suggest that in a given configuration, signal amplification depends primarily on the relative positions of the particles resonance frequencies, rather than on their geometry.

In all configurations in Fig. 4, we find that shifts in the individual resonant frequencies of the interacting particles with respect to the isolated cases are small. Furthermore, these shifts always occur towards smaller frequencies for amplified peaks and towards higher frequencies for attenuated peaks. In addition, we note that both amplification and attenuation occur on the low-frequency side of a given peak. Based on the driven oscillator model, one possible explanation is the following: For the amplified peaks, moving towards higher energies entails a greater phase difference between the oscillators, which leads to destructive interference. Therefore, the resonance can only be amplified at low frequencies. In contrast, for the attenuated peaks, higher energies entail a complete dephasing, but the amplitude of the dephased oscillator becomes small and has little impact on the peak of the resonant oscillator. Thus, the peaks appear to be more attenuated on the low frequency side.

In a three-cylinder configuration, the linewidths remain relatively narrow,[21] and it is possible to distinguish the signal emitted by each individual particle. Furthermore, we find that we can achieve selective amplification with particles that have different resonant frequencies—the cylinder with highest frequency will amplify the signals of the other two. A device that incorporates nanorods with different resonance frequencies can be used as an antenna[25] or as a molecule-specific biological sensor. Thus the cylinders in Fig. 1 make good candidates for such applications because their resonances depend on length as well as diameter. In fact, in Fig. 5 we investigate the response of systems formed by two identical cylinders, one above the other, under different incidence conditions and the behavior of the system is similar to that of a nanoantenna.[25] Now the peak in the scattering intensity of the system of two cylinders is slightly shifted towards smaller photon energies and is broader and larger than that of the isolated 20/80 cylinder spectrum, with near field

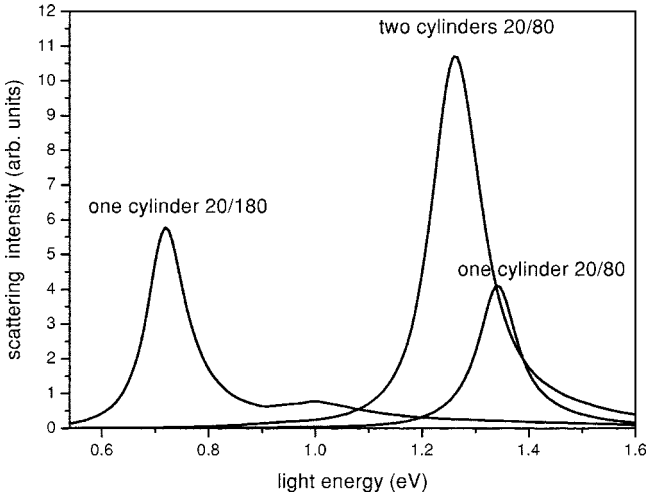

FIG. 5. Light scattering spectra for one cylinder (20/80 in diameter and length, in nm), for two cylinders (20/80) interacting head to head with a separation of 20 nm, and one cylinder (20/180). The index of refraction of the surrounding medium is 1.5.

enhancements in the gap between cylinders. The comparison with the behavior of a single long cylinder with the same diameter (20 nm) and length equal to the sum of the lengths of the small cylinders and the gap between them (180 nm), shows that diffraction and boundary effects in the system formed by two cylinders is very significant in terms of the scattered intensity, while the frequency of the plasmon surface resonance is determined mainly by the size of the individual cylinders.

IV. FIELD AMPLIFICATION COMBINING SPHERES AND NANORODS

We next analyze the ensemble of two spheres with one cylinder. In Fig. 6(a), the cylinder is placed in the middle of a 150 nm sphere and a 60 nm sphere, while in Fig. 6(b), we place a 40 nm sphere between the cylinder and the 150 nm sphere with a separation of 20 nm. In both of these cases we achieve a striking amplification — the cylinders signal is enhanced by a factor of approximately 4, while at the resonance of the large sphere, the signal is 6 times stronger. We anticipate the amplification for the cylinder as explained above by the driven oscillator model. In this case, however, we observe a dramatic field enhancement over a much longer range of frequencies. We believe that this is because the smaller spheres have resonances within the linewidth of the large sphere, which produces a pronounced cooperative effect between these particles leading to a drastic amplification over a broad range of frequencies. This suggests that the large sphere is able to excite the smaller spheres significantly even when it is not directly next to them. However, the overlapping resonances and the broader linewidths of the spheres make it more difficult to identify the individual signals in a multi-particle configuration. In Fig. 6 we indicate with arrows both the maximum (a) and inflection point (b) in the ensemble scattering spectrum that coincide with the resonances of each of the small isolated spheres.

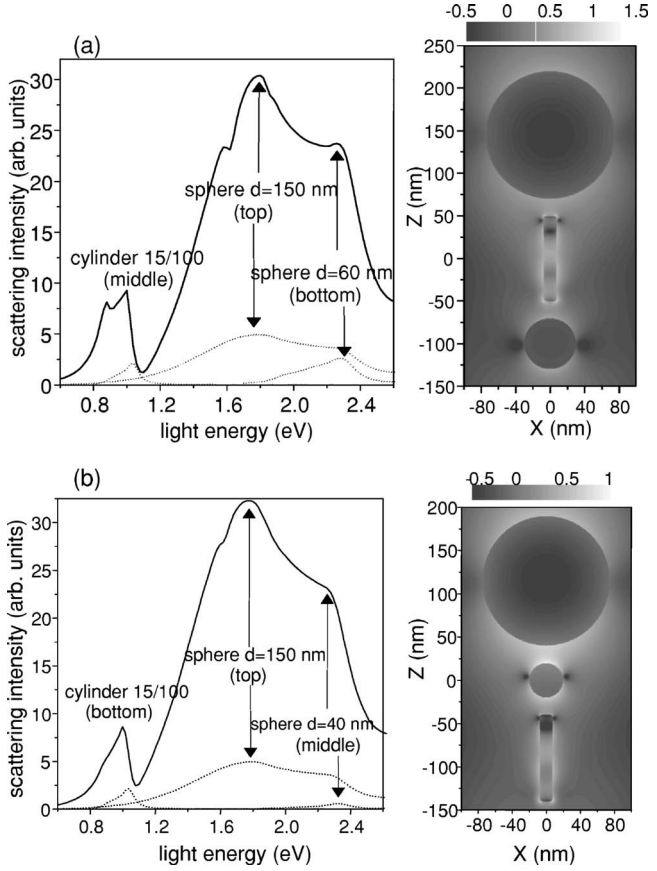

FIG. 6. Left: Light scattering spectra for two spheres and one cylinder (15/100) interacting with a separation of 20 nm (solid line) and spectra of each particle isolated (dotted). Diameter of spheres: (a) 150 and 60 nm; (b) 150 and 40 nm. Right: Distribution of $\log|\mathbf{E}/E_0|$ where $\mathbf{E}$ is the scattered field at $y=0$ for the resonance frequency of the large sphere: 1.8 and 1.78 eV for the (a) and (b) cases, respectively. The index of refraction of the surrounding medium is 1.5.

Figure 6 also includes calculations of the scattered field at $y=0$ (the equatorial plane of the particles), for the two configurations on the left. We use an incident frequency of 1.8 eV in (a) and 1.78 eV in (b). This calculation shows that the large sphere is able to effectively excite the other two particles. We note the concentrations of the field in the areas between the particles. In Fig. 6(a), the cylinder appears to "transmit" the signal between the two spheres. Also, we see that the field penetrates into the cylinder causing an interference pattern. This further supports the ideas presented in the previous section for cylinders of similar dimensions.

V. SELF-SIMILAR SET OF NANOSPHERES

Let us now study a system formed by three silver spheres placed in vacuum whose sizes follow a selfsimilar law, being the radius of the nth sphere 1/3 of the radius of the $(n-1)$th sphere, as proposed in Ref. 17. The configuration of the system is given in the insets in Fig. 7. The results obtained in Ref. 17 predict a large enhancement of the local field between the smallest nanospheres, for energies of 3.25

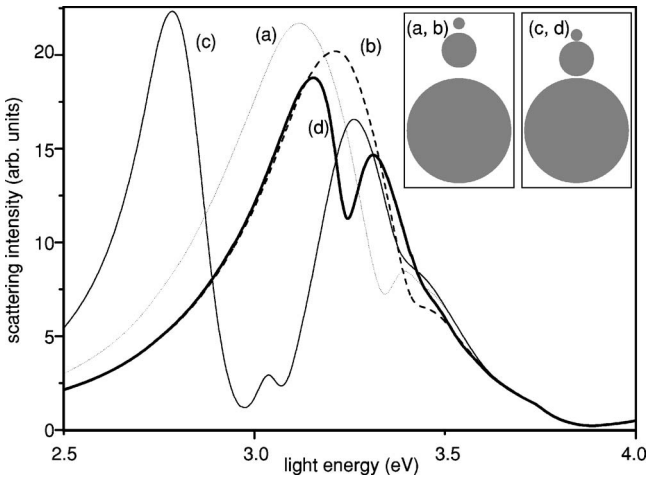

FIG. 7. Far-field scattering amplitude of the system appearing in the insets through an incident plane wave. The wave vector is perpendicular to the symmetry axis of the three-silver-sphere ensemble placed in vacuum in all cases. In (a) and (c) the electric field is oriented perpendicularly to that axis, while in (b) and (d) the electric field is parallel to the symmetry axis. The sphere radii are 45, 15, and 5 nm.

and 3.37 eV, and a large enhancement at the apex on top of the smallest one. Our calculations show that the plasmon resonance frequencies for the isolated spheres are 3.22, 3.46 and 3.50 eV for the biggest, intermediate and smallest sphere, respectively.

We first observe an expected effect: the resultant electromagnetic field strongly depends on the characteristics of the source. In Fig. 7 we show the scattering amplitude of the ensemble of the three silver spheres for two different polarizations of the incoming plane wave which is incident from the lateral direction. In (a) and (b), we have a separation of 9 nm between the large and medium spheres, and 3 nm between the medium and small spheres, and in (c) and (d) we decrease the respective separations to 1.5 and 0.5 nm. We find that the effect of coupling is small, and the peak corresponding to the plasmon resonance of the biggest sphere is dominant. Nevertheless, it is important to note that the situation is different depending on the orientation of the electric field vector; when it is perpendicular to an imaginary line which connects the centers of the spheres [case (a)], the result is qualitatively the same regardless of the orientation of the wave vector; but if it is parallel to such a line, the effects are completely different. In this figure, only results for incidence perpendicular to that line are shown.

If the separation between the spheres becomes smaller (1.5 and 0.5 nm), then the coupling between the modes of the individual spheres grows higher, and some new resonance frequencies are observed. Notice that this result is different from the one appearing in the previous section, where the magnitude of the scattering amplitude increased due to the presence of several particles, but the resonance frequency shifted only slightly. Particularly significant is the case in Fig. 7(c), in which a new peak appears at a frequency which is considerably lower than the individual plasmon resonance of each sphere.

Once we identify the resonance points, the next step is to calculate the value of the local electric field and look for an enhancement similar to the one found in Ref. 17. First we will study the case in which the incident field is perpendicular to the symmetry axis of the system. Figure 8 shows the normalized electric field modulus for both light polarizations on the equatorial plane of the spheres. When the electric vector is perpendicular to the symmetry axis [Fig. 8(a)] the field reaches its maximum value inside the spheres, and de-

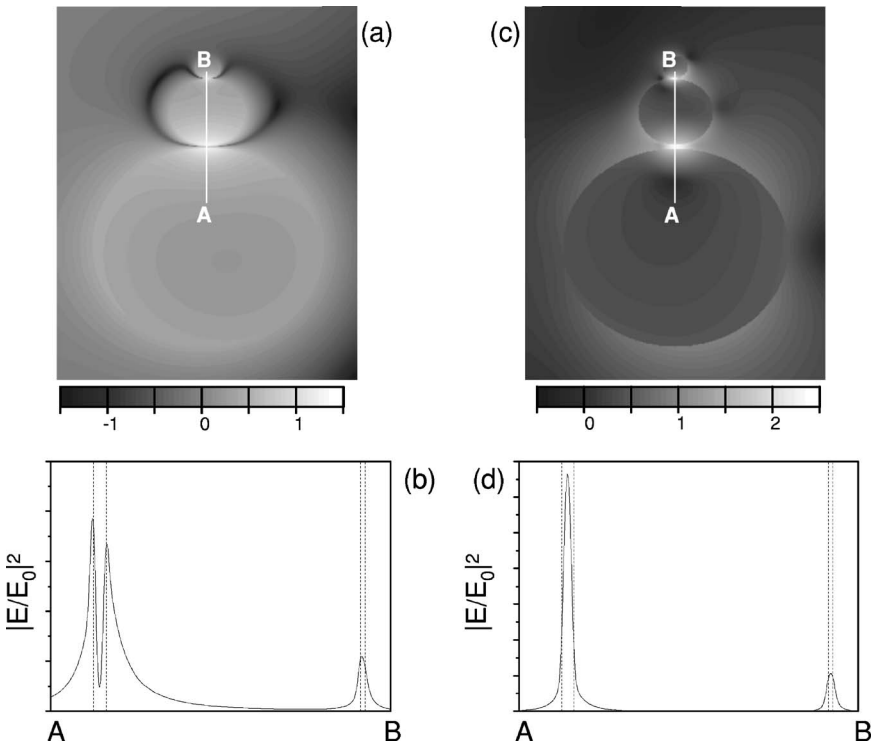

FIG. 8. (a) $\log|\mathbf{E}/E_0|$ for the case (c) of Fig. 7, for the resonance frequency 3.16 eV, in the equatorial plane of the spheres. (b) $|\mathbf{E}/E_0|^2$ for a region of the symmetry axis of the system. The dashed vertical lines are placed in the positions of the sphere surfaces. (c) and (d) Same as (a) and (b), but for the case (d) of Fig. 7 and the resonance frequency 3.26 eV.

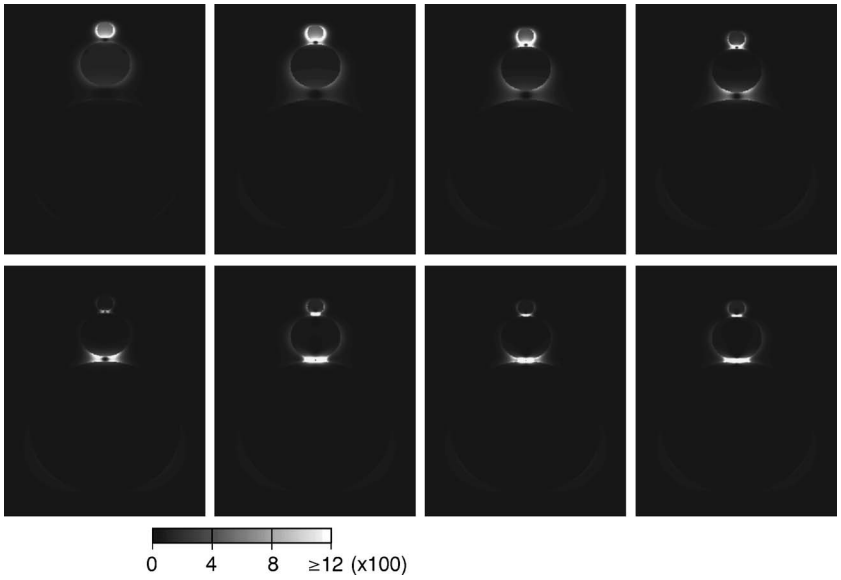

FIG. 9. $|\mathbf{E}/E_0|^2$ for the case of a plane wave coming towards the big sphere from below, given a configuration similar to the ones in Fig. 7, in the equatorial plane of the spheres. The distances between the spheres are decreasing from left to right and from top to bottom.

cays with depth due to the metallic properties of the material. But if the electric vector orientation is parallel to the symmetry axis [Fig.8(b)], then the maximum value of the field intensity occurs between the spheres, which is the desired effect for practical purposes. Compared to the result reported in Ref. 17, the field enhancement we see here is much stronger between the biggest and the intermediate spheres, but weaker between the intermediate and the smallest spheres. We can deduce from these results that the behavior of the system is strongly dependent on the incidence wave vector direction, and therefore the study of the eigenmodes by just solving the homogeneous wave equation is not enough on its own to provide full information about the interaction between this system and light.

Let us study now the case of incidence parallel to the symmetry axis of the system. We choose the incident photon energy corresponding to the frequency of the maximum scattering intensity in Fig. 7(a). The value of the electric field shown at the left top of Fig. 9 exhibits the typical characteristics for a wide range of frequencies around this particular one, when the wave is incident from the bottom of the figure: the field concentrates around the small sphere, and reaches its maximum inside its surface. Of course, it cannot penetrate further, because of the metallic nature of the material. But if we progressively decrease the distances between the spheres (Fig. 9, from left to right and top to bottom), two main features of the electric field appear: first, there is a significant enhancement of the electric field in the regions between the spheres, but there is a minimum of the field intensity which lies exactly in the line which goes from one center to the other, and equidistant from the surface of each sphere. This can be a result of a destructive multiple interference of the waves reflected by the surface of both spheres, causing an effect similar to that of the field emitted by an electric dipole, which cannot propagate in the direction parallel to the source. This behavior was not predicted in Ref. 17, so it must be caused by the interaction of the sphere ensemble with the external field.

VI. SUMMARY AND CONCLUSIONS

In this work we have made a theory and calculations on the response of sets of a few nanocylinders and nanospheres to light in the proximities of the plasmon resonance excitation wavelength. In terms of the spectral lineshapes and spatial intensity near field distribution, we have analyzed and interpreted the collective behavior of the set of cylinders and spheres in comparison with that of the corresponding isolated particles for cases that were previously addressed in experiments. In particular, we have also considered configurations in which the set emits like a nanoantenna. Furthermore, depending on the propagation direction and polarization of the incident wave, we have discussed the possibilities of plasmon polariton excitation and their consequences for near field enhancements and focusing in chains of selfsimilar metallic nanospheres for which the existence of surface eigenmodes were previously predicted by analytically solving the homogeneous problem (namely, no incident wave).

ACKNOWLEDGMENTS

This work has been supported by the European Union, VI Framework Program, and by the Spanish DGICYT. S.E.S. acknowledges support from the Fulbright Commission. L.A.B. is supported by the European Union.

*Electronic address: sburlan@usc.edu
†Electronic address: lablanco@icmm.csic.es
‡Electronic address: mnieto@icmm.csic.es

[1] K. Kneipp, Y. Wang, H. Kneipp, L. T. Perelman, I. Itzkan, R. R. Dasari, and M. S. Feld, Phys. Rev. Lett. **78**, 1667 (1997).
[2] A. Hartschuh, E. J. Sánchez, X. S. Xie, and L. Novotny, Phys. Rev. Lett. **90**, 095503 (2003).
[3] G. Schider, J. R. Krenn, W. Gotschy, B. Lamprecht, H. Ditlbacher, A. Leitner, and F. R. Aussenegg, J. Appl. Phys. **90**, 3825 (2001).
[4] G. Laurent, N. Félidj, J. Aubard, G. Lévi, J. R. Krenn, A. Hohenau, G. Schider, A. Leitner, and F. R. Aussenegg, Phys. Rev. B **71**, 045430 (2005).
[5] J. P. Kottman and O. J. F. Martin, Opt. Lett. **26**, 1096 (2001).
[6] H. Xu, J. Aizpurua, M. Käll, and P. Apell, Phys. Rev. E **62**, 4318 (2000).
[7] K. Kneipp, H. Kneipp, I. Itzkan, R. R. Dasari, and M. S. Feld, J. Phys.: Condens. Matter **14**, R597 (2002).
[8] J. Malicka, I. Gryczynski, C. D. Geddes, and J. R. Lakowicz, J. Biomed. Opt. **8**, 472 (2003).
[9] N. G. Khlebtsov, A. G. Melnikov, L. A. Dykman, and V. A. Bogatyrev, in *Photopolarimetry in Remote Sensing*, edited by G. Videen, Y. Yatskiv, and M. Mishchenko, NATO Science Series Vol. 161 (Plenum, New York, 2004).
[10] A. J. Haes and R. P. Van Duyne, Expert Rev. Mol. Diagn. **4**, 527 (2004).
[11] X. Gao, Y. Cui, R. M. Levenson, L. W. K. Chung, and S. Nie, Nat. Biotechnol. **22**, 969 (2004).
[12] M. Quinten, A. Leitner, J. R. Krenn, and F. Ausseneg, Opt. Lett. **23**, 1331 (1998).
[13] S. I. Bozhevolnyi, J. Erland, K. Leosson, P. M. W. Skovgaard, and J. M. Hvam, Phys. Rev. Lett. **86**, 3008 (2001).
[14] R. Quidant, C. Girard, J. C. Weeber, and A. Dereux, Phys. Rev. B **69**, 085407 (2004).
[15] N. Calander and M. Willander, Phys. Rev. Lett. **89**, 143603 (2002).
[16] H. Xu and M. Käll, Phys. Rev. Lett. **89**, 246802 (2002).
[17] K. Li, M. I. Stockman, and D. J. Bergman, Phys. Rev. Lett. **91**, 227402 (2003).
[18] H. C. Vand de Hulst, *Light Scattering by Small Particles* (Dover, New York, 1981).
[19] M. Kerker, *The Scattering of Light and Other Electromagnetic Radiation* (Academic Press, New York, 1969).
[20] J. Prikulis, H. Xu, L. Gunnarsson, M. Käll, and H. Olin, J. Appl. Phys. **92**, 6211 (2002).
[21] C. Sönnichsen, T. Franzl, T. Wilk, G. von Plessen, J. Feldmann, O. Wilson, and P. Mulvaney, Phys. Rev. Lett. **88**, 077402 (2002).
[22] F. J. García de Abajo and A. Howie, Phys. Rev. Lett. **80**, 5180 (1998); Phys. Rev. B **65**, 115418 (2002).
[23] E. D. Palik, *Handbook of Optical Constants of Solids* (Academic Press, San Diego, 1985).
[24] C. F. Bohren and D. R. Huffman, *Absorption and Scattering of Light by Small Particles* (John Wiley & Sons, New York, 1998).
[25] P. Mühlschlegel, H. J. Eisler, O. J. F. Martin, B. Hecht, and D. W. Pohl, Science **308**, 1607 (2005).
[26] M. Quinten, A. Pack, and R. Wannemacher, Appl. Phys. B **68**, 87 (1999).